VISUALIZING PARAMETRIC SOLUTION SETS*

E. D. POPOVA[1] and W. KRÄMER[2],**

[1]*Institute of Mathematics and Informatics, Bulgarian Academy of Sciences,
Acad. G. Bonchev str., bl. 8, 1113 Sofia, Bulgaria. email: epopova@bio.bas.bg*

[2]*Faculty of Mathematics and Natural Sciences, University of Wuppertal, Gaußstr. 20,
42119 Wuppertal, Germany. email: kraemer@math.uni-wuppertal.de*

Abstract.

We characterize the boundary $\partial \Sigma^p$ of the solution set Σ^p of a parametric linear system $A(p)x = b(p)$ where the elements of the $n \times n$ matrix and the right-hand side vector depend on a number of parameters p varying within interval bounds. The characterization of $\partial \Sigma^p$ is by means of pieces of parametric hypersurfaces, the latter represented by their coordinate functions depending on corresponding subsets of $n-1$ parameters. The presented approach has a direct application for efficient visualization of parametric solution sets by utilizing some plotting functions supported by *Mathematica* and Maple.

Electronic Supplementary Material: The online version of this article (doi:10.1007/ s10543-007-0159-3) contains supplementary material, which is available to authorized users.

1 Introduction.

Consider the linear algebraic system

$$(1.1) \qquad A(p) \cdot x = b(p),$$

where the elements of the $n \times n$ matrix $A(p)$ and the vector $b(p)$ are affine-linear functions

$$(1.2) \qquad a_{ij}(p) := a_{ij,0} + \sum_{\nu=1}^{k} a_{ij,\nu} p_\nu, \quad b_i(p) := b_{i,0} + \sum_{\nu=1}^{k} b_{i,\nu} p_\nu,$$

$$a_{ij,\nu}, b_{i,\nu} \in \mathbb{R}, \quad \nu = 0, \ldots, k, \ i,j = 1, \ldots, n$$

of k parameters. The parameters are considered to be uncertain and varying within given intervals

$$(1.3) \qquad p \in [p] = ([p_1], \ldots, [p_k])^\top.$$

Such systems are common in many engineering analysis or design problems, models in operational research, linear prediction problems, etc., where there are complicated dependencies between the coefficients of the system [1, 2, 14]. The uncertainties in the model parameters could originate from an inexact knowledge of these parameters, measurement imprecision, or round-off errors. Linear systems with interval input data are applicable also to uncertainty theories which rely on interval arithmetic for computations, such as fuzzy set theory, random set theory, or probability bounds theory.

The set of solutions to (1.1–1.3), called parametric solution set, is

$$(1.4) \qquad \Sigma^p = \Sigma(A(p), b(p), [p]) := \{x \in \mathbb{R}^n \mid \exists p \in [p], A(p)x = b(p)\}.$$

The well-known non-parametric interval linear system $[A]x = [b]$, which is the most studied in the interval literature, can be considered as a special case of the parametric linear system with $n^2 + n$ independent parameters $a_{ij} \in [a_{ij}]$, $b_i \in [b_i]$, $i,j = 1, \ldots, n$. For a parametric system (1.1–1.3), the corresponding non-parametric one with $[A] = ([a_{ij}]) \in \mathbb{IR}^{n \times n}$, $[b] \in \mathbb{IR}^n$ can be obtained as

$$[a_{ij}] = a_{ij,0} + \sum_{\nu=1}^k a_{ij,\nu}[p_\nu], \quad [b_i] = b_{i,0} + \sum_{\nu=1}^k b_{i,\nu}[p_\nu], \ i,j = 1, \ldots, n.$$

The non-parametric solution set, called also united solution set, is defined as

$$\Sigma([A], [b]) := \{x \in \mathbb{R}^n \mid \exists A \in [A], \ \exists b \in [b], \ A \cdot x = b\}.$$

In general, $\Sigma(A(p), b(p), [p]) \subseteq \Sigma([A], [b])$ since the elements of $[A]$, $[b]$ are perturbed independently in contrast to $A(p)$, $b(p)$ with $p \in [p]$. Figure 3.1B illustrates both solution sets for the system from Example 3.1 and some of their properties. The parametric solution set Σ^p is smaller and much more complicated than the corresponding non-parametric solution set. For example, Σ^p is generally not convex even in a single orthant. Therefore, it would be interesting and helpful to see how some parametric solution sets look like. The visualization of Σ^p (even only in 2D or 3D) would be helpful not only for graphical illustration but also for exploration of some properties and for comparison of some numerical results.

In a series of papers (see e.g. [4, 5, 6] and the references therein) Alefeld, Kreinovich, and Mayer give various descriptions of the solution sets for systems of interval linear equations with dependent coefficients, paying particular attention to the symmetric solution set. For example, in [5] the parametric solution set is described as a semialgebraic set. Unfortunately, most of these descriptions do not contain a constructive process which could be used for drawing the parametric solution set. This gap was filled in [7] where the solution sets of parametric linear systems involving affine-linear dependencies were characterized by

systems of inequalities obtained by a Fourier–Motzkin like elimination process. Provided that the proposed Fourier–Motzkin like elimination process is implemented in suitable software tools, this approach can be applied for drawing the parametric solution sets in environments supporting tools for inequalities plotting. The algorithms for plotting inequalities are usually based on cylindrical algebraic decomposition (CAD) [9]. Although CAD is an algorithmic process, it becomes computationally infeasible for complicated inequalities.

Utilizing the set of inequalities by which the famous Oettli–Prager theorem [15] characterizes the non-parametric solution set and the tools for inequalities plotting supported in *Mathematica* [20], corresponding functions for drawing non-parametric solution sets in 2D and 3D were developed and a suitable web interface to these functions was provided [18]. Recently some tools for drawing non-parametric and connected parametric solution sets were also reported [12, 18]. The visualization function reported in [18] utilizes the available *Mathematica* functions for plotting parametric curves but the quality of the produced solution set image has some deficiencies.

In this paper we present an approach for characterizing the parametric solution set which is alternative to that based on systems of inequalities [7]. Our approach is designed particularly for visualization of the parametric solution set boundary and can be easily implemented in the environments of *Mathematica* [20] and Maple [11] which support functions for plotting parametric curves and surfaces. Section 3 discusses how to utilize the plotting functions in *Mathematica* and Maple for visualization the solution sets of some special cases of parametric linear systems. In Section 4 we derive our approach and characterize the boundary $\partial \Sigma^p$ of the solution set Σ^p to a system involving affine-linear dependencies by means of pieces of parametric hypersurfaces, the latter represented by their coordinate functions depending on corresponding sets of $n-1$ parameters. The numerical examples, given throughout the paper and in Section 5, demonstrate the discussed visualization approaches and illustrate some properties of the parametric solution sets.

2 Preliminaries.

Denote by $\mathbb{R}^n, \mathbb{R}^{n \times m}$ the set of real vectors with n components and the set of real $n \times m$ matrices, respectively. A real compact interval is $[a] = [a^-, a^+] := \{a \in \mathbb{R} \mid a^- \le a \le a^+\}$. By $\mathbb{IR}^n, \mathbb{IR}^{n \times m}$ we denote the sets of interval n-vectors and interval $n \times m$ matrices, respectively. The end-point functionals $(\cdot)^-, (\cdot)^+$ are applied to interval vectors and matrices componentwise.

PROPOSITION 2.1. *If $A(p)$ is nonsingular for all $p \in [p]$ then Σ^p is compact and connected.*

PROOF. Since $A(p)$ is non-singular for every $p \in [p]$, $A^{-1}(p)$ exists for $p \in [p]$ and $x(p) := A^{-1}(p) \cdot b(p)$ is a function of k variables $p \in \mathbb{R}^k$ which is continuous. Since $[p_\nu], \nu = 1, \ldots, k$ are connected and compact, the same holds for the image Σ^p of $x(p)$. □

An obvious set-theoretical description of the parametric solution set is given by the following

PROPOSITION 2.2.

$$\Sigma^p(A(p), b(p), [p]) := \bigcup_{\tilde{p} \in [p]} \{x \in \mathbb{R}^n \mid A(\tilde{p}) \cdot x = b(\tilde{p})\}.$$

In particular, if $A(p)$ is square nonsingular for all $p \in [p]$ then

$$\Sigma^p(A(p), b(p), [p]) := \bigcup_{\tilde{p} \in [p]} \{x(\tilde{p}) = A^{-1}(\tilde{p}) \cdot b(\tilde{p})\}.$$

Denote by $\partial \Sigma^p$ the boundary of the parametric solution set Σ^p. In what follows we will characterize $\partial \Sigma^p$ by pieces of parametric hypersurfaces. In algebraic geometry, a hypersurface in n-dimensional projective space is an algebraic surface of dimension $(n-1)$. It is then defined by a single equation

$$f(x_1, \ldots, x_n) = 0,$$

a homogeneous polynomial in the homogeneous coordinates. Hypersurface is a special name for a submanifold of codimension one [19]. The function above may have singularities and thus it may not be a submanifold in the strict sense. The definitions of hypersurfaces may differ depending on exactly which properties are required, see e.g. [3] for a definition of real analytic hypersurfaces.

DEFINITION 2.1. *A hypersurface in n-dimensional space is called* parametric *if it is defined by n coordinate functions*

$$x_i = x_i(p_1, \ldots, p_k), \quad i = 1, \ldots, n$$

depending on $k = n - 1$ parameters.

Parametric hypersurface (PHS) is then a hypersurface whose coordinate functions are parameterized. Here we will consider parametric hypersurfaces, denoted by n-dimensional vectors $x(p)$, where p is a $n-1$-dimensional parameter vector, which are defined by the analytic solution of parametric linear systems (1.1–1.3). For simplicity, a k-dimensional C^m-surface in $\mathbb{R}^n$, where $m \geq 1$ and $k < n-1$, will be called degenerate parametric hypersurface. In a 3D space degenerate parametric hypersurfaces are curves and points, see Figure 3.2B e.g., or Figure 4.2A and B.

Particular pieces (parts) of a parametric hypersurface will be obtained for specified ranges of the parameters $p_j^- \leq p_j \leq p_j^+$, $j = 1, \ldots, k$. Therefore, particular parts of a parametric hypersurface will be denoted by $x(p)|_{p \in [p]}$ and will be also called restricted PHS-s.

3 Special cases.

In this section we demonstrate how to utilize the plotting functions in *Mathematica* and Maple for visualizing the solution set of some particular cases of 2D and 3D parametric linear systems.

Consider the parametric linear system (1.1–1.3). If $A(p)$ is nonsingular for all $p \in [p]$ and the number of parameters is $k \leq n - 1$, then $x(p) = A^{-1}(p) \cdot b(p)$ defines a PHS (curve for $k = 1$) in $\mathbb{R}^n$ which fully characterizes the parametric solution set (1.4), respectively its boundary.

For $n = 2$, $k = n - 1$, e.g., the parametric solution set is a parametric curve whose x, y coordinates are functions of one uncertain parameter $p \in [p]$

$$x = x_1(p) = \{A^{-1}(p) \cdot b(p)\}_1$$
$$y = x_2(p) = \{A^{-1}(p) \cdot b(p)\}_2.$$

Many computer algebra systems, e.g. *Mathematica* [20] and Maple [11] have built-in functions for drawing 2D and 3D parametric plots. In 2D, *Mathematica* and Maple effectively generate a sequence of points by varying the parameter p, then form a curve by joining these points.

EXAMPLE 3.1. *(n = 2, k = 1) Let*

$$A(p) = \begin{pmatrix} 3p & 1 \\ -2 & 3p - 1 \end{pmatrix}, \quad b(p) = \begin{pmatrix} 2p \\ p \end{pmatrix}, \quad p \in [0, 1].$$

For these data, the parametric solution set is that part of the parametric curve

$$x(p) = A^{-1}(p) \cdot b(p) = \begin{pmatrix} -3p + 6p^2 \\ 4p + 3p^2 \end{pmatrix} / (2 - 3p + 9p^2)$$

which is obtained for $0 \leq p \leq 1$.

The following Maple code visualizes in Figure 3.1A the parametric solution set as a part of the corresponding parametric curve.

```
> A:=[[3*p, 1], [-2, 3*p-1]]:
> b:=[2*p, p]:
> x:=linalg[linsolve](A, b):
> plot([x[1], x[2], p=0..1]);
```

The same figure can be generated in *Mathematica* by using its kernel function `ParametricPlot`.

Mathematica and Maple can be also used for plotting either one- or two-parameter sets of points in a 3D space. The built-in functions `plot3D` in Maple or `ParametricPlot3D` in *Mathematica* create three-dimensional space curves and surfaces, parameterized by one or two coordinates respectively. In *Mathematica* the surface is formed from a collection of quadrilaterals. The corners of the quadrilaterals have coordinates corresponding to the values of $z = z(u, v)$ when the parameters u and v take on values in a regular grid. The option `PlotPoints` of the *Mathematica* function `ParametricPlot3D` allows a user to specify the number of sample points used. The *Mathematica* package `Graphics'ParametricPlot3D'` extends the kernel function `ParametricPlot3D` by providing an alternative to the `PlotPoints` option where the sampling may
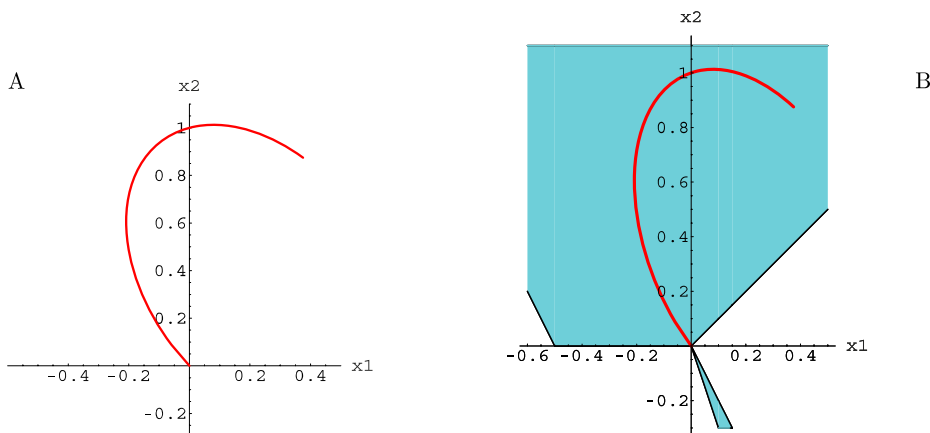
Figure 3.1: A: The parametric solution set of the system from Example 3.1; B: Both the parametric solution set and part of the corresponding non-parametric solution set.

be specified by giving a step size in each coordinate. The package also introduces `PointParametricPlot3D` function for plotting either one- or two-parameter sets of points in space.

EXAMPLE 3.2. *(n = 3, k = 2) Let*

$$A(p) = \begin{pmatrix} 1 & p & q \\ p & 2 & p \\ q & p & 3 \end{pmatrix}, \quad b(p) = \begin{pmatrix} 1 \\ p^2 \\ q^2 \end{pmatrix}, \quad \begin{array}{l} p \in [0,1] \\ q \in [0,0.9]. \end{array}$$

The following *Mathematica* code generates the snail represented in Figure 3.2A.

```
In[1]:= A = {{1,p,q}, {p,2,p}, {q,p,3}};
        b = {1, p^2, q^2};
        x = LinearSolve[A, b];
        ParametricPlot3D[x, {p,0,1}, {q,0,0.9}];
```

EXAMPLE 3.3. *(n = 3, k = 1) For*

$$A(p) = \begin{pmatrix} 1 & p & p \\ p & 2 & p \\ p & p & 3 \end{pmatrix}, \quad b(p) = \begin{pmatrix} 1 \\ p^2 \\ p^2 \end{pmatrix}, \quad p \in [-0.2, 0.1],$$

the one-parameter solution set is a 3D curve represented in Figure 3.2B.

For 2D systems involving more than one parameter and having nonsingular matrices for all values of the parameters, we can get a good impression of the parametric solution set by drawing a set of one-parameter curves obtained for the parameters after the first one taking on values in a grid of points within the parameter intervals. This approach is implemented in a *Mathematica* function
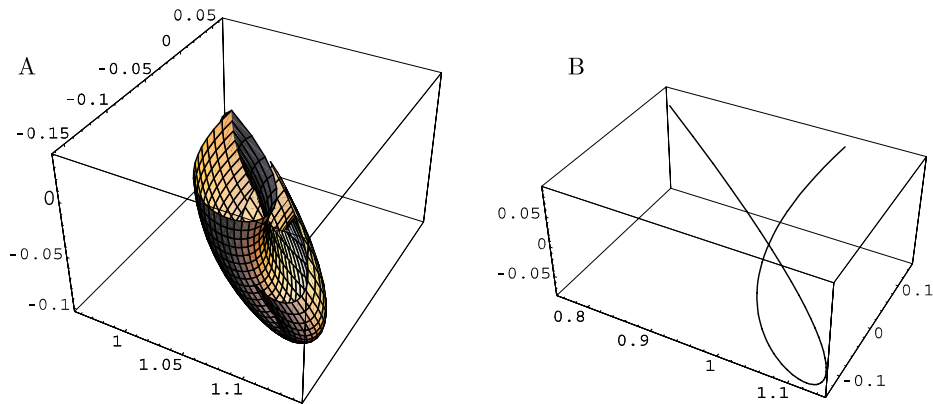
Figure 3.2: One- (B) and two-parameter (A) solution sets corresponding to the 3D linear systems from Examples 3.3 and 3.2, respectively.

ParametricSSet which is part of the package **IntervalComputations'Solution Sets'**. The following Example illustrates the usage of this function.

EXAMPLE 3.4. *(n = 2, k = 2) Let*

$$A(p) = \begin{pmatrix} p & q-1 \\ q & p \end{pmatrix}, \quad b(p) = \begin{pmatrix} -q+1/3 \\ q \end{pmatrix}, \quad p \in [-2, -1], \ q \in [3, 5].$$

The following *Mathematica* code first loads the package, then defines the arguments and calls the visualization function.

```
In[5]:= << IntervalComputations'SolutionSets'
In[6]:= A = {{p, q-1}, {q, p}};b={-q+1/3, q};
        tr = {p->Interval[{-2, -1}],  q->Interval[{3, 5}]};
        ParametricSSet[A, b, tr];
```

The function **ParametricSSet[mat, vec, tr]** has three obligatory arguments: **mat** is the parametric matrix of the system, **vec** is the right-hand side vector, and **tr** is a list of *Mathematica* rules specifying the parameters and their interval values. By default, **ParametricSSet** draws a set of one-parameter curves taken on an uniform mesh in the parameter intervals after the first one. The default value for the mesh step size is 1% of the interval width. Figure 3.3A represents the generated graphics image.

By an optional argument **StepSize**, one can specify particular values for the step size of all parameter values after the first one. The graphics in Figure 3.3B is drawn by specifying **StepSize->{0.1}** regarding the second parameter **q**. Although the set of one-parameter curves in Figure 3.3B is more shaggy than that in Figure 3.3A, the shape of the parametric solution set is still well visible.

```
In[9]:= tr = {q->Interval[{3, 5}],  p->Interval[{-2, -1}]};
        ParametricSSet[m, b, tr, StepSize->{0.05}];
```
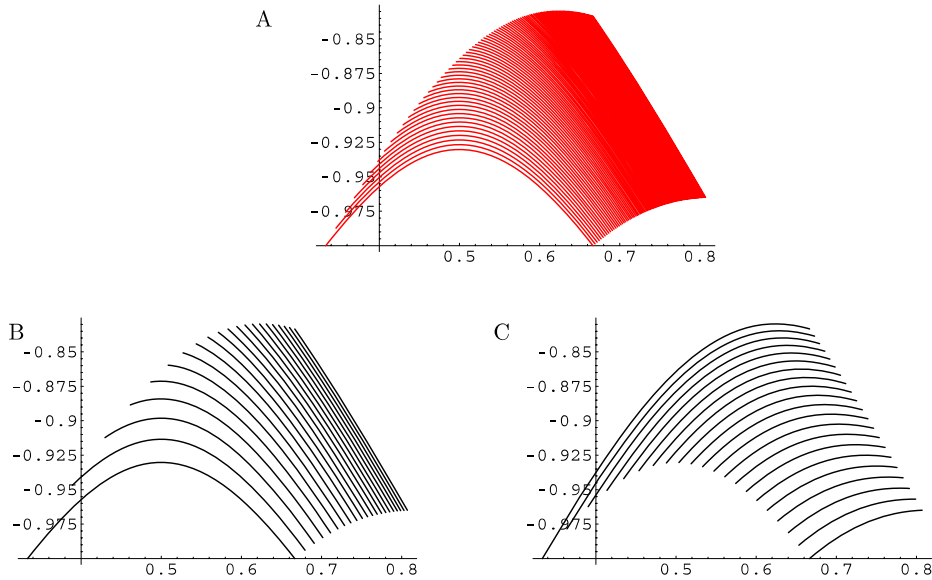
Figure 3.3: The parametric solution set of Example 3.4 built by 1-parameter curves drawn on an uniform mesh for the parameters after the first one. A: the default value for the `StepSize` which is 1% of the interval width, B: `StepSize`= 0.1 for the parameter q, C: `StepSize`= 0.05 for the parameter p.

One can change the order in which the parameters are enlisted in the third argument of the function `ParametricSSet`, and this way to represent the parametric solution set by another set of one-parameter curves. The result of the execution of the above code can be seen in Figure 3.3C.

Based on the representation given by Proposition 2.2, a 2D parametric solution set can be visualized by a set of one-parameter curves drawn in a mesh of values for the parameters after the first one. This is the only approach for visualization the solution set of a 2D linear system involving nonlinear dependencies. Unfortunately, the above approach is not applicable for drawing disconnected 2D solution sets and in the case of 3D systems. An important disadvantage is the big size of the graphics image which increases with decreasing the mesh step size. That is why, in the next section we derive another approach for visualization only the boundary of the parametric solution set. To this end, the parametric solution set is characterized by parametric hypersurfaces.

4   Main results.

Let $\mathcal{K} = \{1, \ldots, k\}$. For $n \leq k$, define $Q(n - 1, k)$ as the set of all possible subsets of $\mathcal{K}$ containing $n - 1$ elements

$$Q(n - 1, k) := \{q = \{i_1, \ldots, i_{n-1}\} \mid q \subset \mathcal{K}, \ \mathrm{Card}(q) = n - 1\}.$$

For $k < n$, $Q(n-1,k) := \{q \mid q = \mathcal{K}\}$, that is $Q(n-1,k)$ consists of only one set which is the set $\mathcal{K}$ itself. For $n \leq k$ the cardinality of $Q(n-1,k)$ is $\mathrm{Card}(Q(n-1,k)) = \binom{k}{n-1} = \frac{k!}{(k-n+1)!(n-1)!}$. For $q = \{i_1, \ldots, i_{n-1}\} \in Q(n-1,k)$, the vector $(p_{i_1}, \ldots, p_{i_{n-1}})$ will be denoted by p_q.

For a vector $p = (p_1, \ldots, p_k) \in \mathbb{R}^k$ and $q \in Q(n-1,k)$, define $\tilde{q} = \mathcal{K} \setminus q$ and two vectors $p_q \in \mathbb{R}^{n-1}$, $p_{\tilde{q}} \in \mathbb{R}^{k-n+1}$ by

$$p_q := (p_{i_1}, \ldots, p_{i_{n-1}}),$$
$$p_{\tilde{q}} := (p_{i_n}, \ldots, p_{i_k}).$$

For $n \leq k$, the vectors p_q and $p_{\tilde{q}}$ split the original vector p into two nonintersecting subvectors defined by the set of indexes q.

Denote by $U(k-n+1) := \{u \in \mathbb{R}^{k-n+1} \mid |u| = (1, \ldots, 1)^\top\}$ the set of all $(k-n+1)$-dimensional sign vectors, where the absolute value $|u|$ is understood componentwise $|u| := (|u_1|, \ldots, |u_k|)^\top$ for $u \in \mathbb{R}^k$. For $[a] = [a^-, a^+] \in \mathbb{IR}^{k-n+1}$ and $u \in U(k-n+1)$,

$$\{a^u\}_i := \begin{cases} a_i^- & \text{if } u_i = -1 \\ a_i^+ & \text{if } u_i = 1 \end{cases}, \quad i = 1, \ldots, k-n+1.$$

Thus for an interval vector $[a]$, a^u denotes a real vector whose elements are corresponding interval end-points. The number of elements in the set $U(k-n+1)$ is $\mathrm{Card}(U(k-n+1)) = 2^{k-n+1}$.

Let $v \in \mathbb{R}^n$ be a numerical vector. Define a cone

$$K(v) := \big\{(x_1, \ldots, x_n) \in \mathbb{R}^n : x_i \geq 0 \text{ if } \mathrm{sign}(v_i) \geq 0;\ x_i \leq 0 \text{ if } \mathrm{sign}(v_i) \leq 0\big\}.$$

For a fixed $v \in \mathbb{R}^n$, $K(v)$ defines an orthant in $\mathbb{R}^n$. It is obvious that $K(v)$ is a polyhedral cone and therefore it is a closed convex cone. $K(v)$ is solid since the interior of $K(v)$ is not empty. Since $K(v) \cap -K(v) = \{0\}$, $K(v)$ is pointed. Being a pointed, solid, closed convex cone, $K(v)$ is a proper cone [8]. The proper cone $K(v)$ induces a partial ordering in $\mathbb{R}^n$ via

$$y \stackrel{K(v)}{\leq} x \Longleftrightarrow x - y \in K(v).$$

Our first theorem characterizes exactly the boundary $\partial \Sigma^p$ by parts of parametric hypersurfaces in the special case when the number of the parameters is less than or equal to the dimension of the system.

THEOREM 4.1. *If $A(p)$ is nonsingular for all $p \in [p]$ and $k \leq n$, then*

$$\partial \Sigma^p = \bigcup_{q \in Q(n-1,k)} \{x(p_q, p_{\tilde{q}}^-)|_{p_q \in [p_q]},\ x(p_q, p_{\tilde{q}}^+)|_{p_q \in [p_q]}\}.$$

PROOF. By definition, every tuple of $n-1$ parameters determines one parametric hypersurface (PHS) in the n-dimensional space. So, if $k \leq n-1$, $\partial \Sigma^p$

consists of a piece of exactly one PHS, degenerate if $k < n - 1$, which is the parametric solution set itself

$$\partial\Sigma^p = x(p)|_{p \in [p]} = \Sigma^p,$$

where $x(p) = A^{-1}(p) \cdot b(p)$ and $[p] \in \mathbb{IR}^k$, $k \le n - 1$.

Let $k = n$. For a fixed $q \in Q(n-1, k)$, $p_{\tilde{q}}$ is a one-component vector. Define the set of restricted PHS-s

$$\Sigma^{p_q, p_{\tilde{q}}} := \bigcup_{t \in [p_{\tilde{q}}]} x(p_q, t)|_{p_q \in [p_q]}.$$

It is evident that $\Sigma^{p_q, p_{\tilde{q}}} \equiv \Sigma^p$. We have the following equivalent representations of these sets.

$$\Sigma^{p_q, p_{\tilde{q}}} = \left\{ x \in \mathbb{R}^n \mid \exists p_q \in [p_q], \ \exists p_{\tilde{q}} \in [p_{\tilde{q}}], \ A(p_q, p_{\tilde{q}})x = b(p_q, p_{\tilde{q}}) \right\}$$
$$= \left\{ x \in \mathbb{R}^n \mid \exists p_q \in [p_q], \ \exists p_{\tilde{q}} \in [p_{\tilde{q}}], \ A(p_q)x - b(p_q) = p_{\tilde{q}}(b^{p_{\tilde{q}}} - A^{p_{\tilde{q}}}x) \right\},$$

where $A^{p_{\tilde{q}}} \in \mathbb{R}^{n \times n}$, $b^{p_{\tilde{q}}} \in \mathbb{R}^n$, $A^{p_{\tilde{q}}} = \frac{\partial A(p_q, p_{\tilde{q}})}{\partial p_{\tilde{q}}}$, $b^{p_{\tilde{q}}} = \frac{\partial b(p_q, p_{\tilde{q}})}{\partial p_{\tilde{q}}}$, $A(p_q) = A(p_q, p_{\tilde{q}}) - p_{\tilde{q}}A^{p_{\tilde{q}}}$, $b(p_q) = b(p_q, p_{\tilde{q}}) - p_{\tilde{q}}b^{p_{\tilde{q}}}$. For $v = b^{p_{\tilde{q}}} - A^{p_{\tilde{q}}}x$ we obtain

$$\Sigma^{p_q, p_{\tilde{q}}} = \left\{ x \in \mathbb{R}^n \mid \exists p_q \in [p_q], \right.$$
$$\left. p_{\tilde{q}}^-(b^{p_{\tilde{q}}} - A^{p_{\tilde{q}}}x) \overset{K(v)}{\le} A(p_q)x - b(p_q) \overset{K(v)}{\le} p_{\tilde{q}}^+(b^{p_{\tilde{q}}} - A^{p_{\tilde{q}}}x) \right\}.$$

Therefore, the restricted PHS-s $x(p_q, p_{\tilde{q}}^-)|_{p_q \in [p_q]}$, $x(p_q, p_{\tilde{q}}^+)|_{p_q \in [p_q]}$, obtained as solutions of the following parametric systems depending on $n - 1$ parameters p_q

$$(A(p_q) + p_{\tilde{q}}^- A^{p_{\tilde{q}}})x = b(p_q) + p_{\tilde{q}}^- b^{p_{\tilde{q}}}, \quad \text{resp.}$$
$$(A(p_q) + p_{\tilde{q}}^+ A^{p_{\tilde{q}}})x = b(p_q) + p_{\tilde{q}}^+ b^{p_{\tilde{q}}},$$

belong to $\partial\Sigma^{p_q, p_{\tilde{q}}}$. Due to $\Sigma^{p_q, p_{\tilde{q}}} \equiv \Sigma^p$, these end-point PHS-s belong to the boundary of the parametric solution set Σ^p, too. For $q_1, q_2 \in Q(n - 1, k)$, $q_1 \ne q_2$ and fixed $t_1 \in [p_{\tilde{q}_1}]$, $t_2 \in [p_{\tilde{q}_2}]$, in general $x(p_{q_1}, t_1) \ne x(p_{q_2}, t_2)$, but $\Sigma^{p_{q_1}, p_{\tilde{q}_1}} \equiv \Sigma^{p_{q_2}, p_{\tilde{q}_2}}$. Thus, when q traces the set $Q(n-1, k)$, $p_{\tilde{q}}$ traces all the parameters, respectively all the boundary parametric hypersurfaces, which proves the theorem. $\qquad\square$

Figures 3.3B and 3.3C illustrate the above theorem.

REMARK 4.1. If $k = n$ and for some $q_1 \in Q(n - 1, k)$, some $\lambda \in \{-, +\}$, $x(p_{q_1}, p_{\tilde{q}_1}^\lambda)$ is degenerate, then there exist $q_2 \in Q(n - 1, k)$, $\mu \in \{-, +\}$ such that $x(p_{q_2}, p_{\tilde{q}_2}^\mu)$ is non-degenerate and $x(p_{q_1}, p_{\tilde{q}_1}^\lambda) \in x(p_{q_2}, p_{\tilde{q}_2}^\mu)$. See Example 4.2 and Figure 4.2 A, B for an illustration.

EXAMPLE 4.1. *Consider the parametric linear system*

$$\begin{pmatrix} p_1 & p_2 - 1 \\ p_2 & p_1 \end{pmatrix} \cdot x = \begin{pmatrix} -p_2 + 1/3 \\ p_2 \end{pmatrix}, \quad p_1 \in [-2, -1], \quad p_2 \in [3, 5].$$

For $p_1 \in [-2, -1]$, $p_2 \in [3, 5]$, $A(p)$ is nonsingular and

$$A^{-1}(p) = \begin{pmatrix} p_1 & 1 - p_2 \\ -p_2 & p_1 \end{pmatrix} / (p_1^2 + p_2 - p_2^2).$$

We have $Q(n - 1, k) = Q(1, 2) = \{\{1\}, \{2\}\}$. For $q = \{1\}$,

$$x(p_1, p_2^-) = \begin{pmatrix} -2(9 + 4p_1)/3 \\ 8 + 3p_1 \end{pmatrix} / (-6 + p_1^2),$$

$$x(p_1, p_2^+) = \begin{pmatrix} -2(30 + 7p_1) \\ 5(14 + 3p_1) \end{pmatrix} / (-60 + 3p_1^2).$$

For $q = \{2\}$,

$$x(p_2, p_1^-) = \begin{pmatrix} 2 - 9p_2 + 3p_2^2 \\ -p_2(8 - 7 + 3p_2) \end{pmatrix} / (-12 - 3p_2 + 3p_2^2),$$

$$x(p_2, p_1^+) = \begin{pmatrix} 1 - 6p_2 + 3p_2^2 \\ -p_2(-4 + 3p_2) \end{pmatrix} / (-3 - 3p_2 + 3p_2^2).$$

The corresponding parts of the above boundary curves are drawn on Figure 4.1. Compare Figures 4.1 and 3.3.
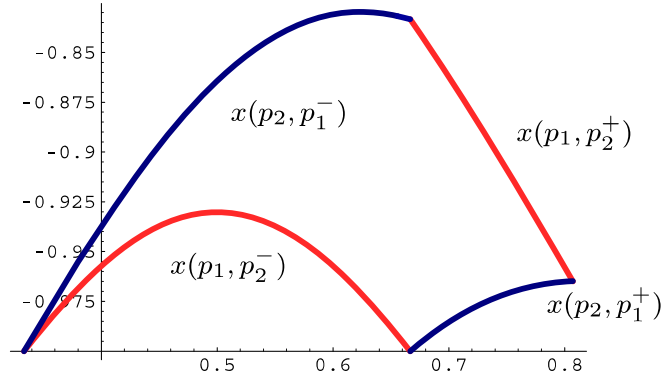

Figure 4.1: Boundary curves for the parametric solution set from Example 4.1.

Let $k > n$ and $q \in Q(n - 1, k)$ be fixed. Since $k > n$, the corresponding "free" parameters $p_{\tilde{q}} \in \mathbb{R}^{k-n+1}$ are more than one. Let $k - n + 1 = 2$. For fixed $t_1 \in \{[p_{\tilde{q}}]\}_1$, define a set of restricted PHS-s

$$\Sigma^{p_q, t_1} := \{x(p_q, t_1, t_2)|_{p_q \in [p_q]} \mid t_2 \in \{[p_{\tilde{q}}]\}_2\}.$$

Then the whole parametric solution set Σ^p can be considered as a family Σ^{p_q} of sets defined by one free parameter

(4.1) $$\Sigma^{p_q} := \bigcup_{t_1 \in \{[p_{\tilde{q}}]\}_1} \Sigma^{p_q, t_1}.$$

By Theorem 4.1, $\partial\Sigma^{p_q,t_1} = \{x(p_q,t_1,t_2^-)|_{p_q\in[p_q]}, x(p_q,t_1,t_2^+)|_{p_q\in[p_q]}\}$, where $t_2 = \{[p_{\bar{q}}]\}_2$. Thus, for $k-n+1=2$ we obtain

$$\partial\Sigma^{p_q} \subseteq \partial\Sigma^{p_q,t_1^\lambda} = \bigcup_{u\in U(k-n+1)} x(p_q,p_{\bar{q}}^u)\big|_{p_q\in[p_q]},$$

where $t_1 \in \{[p_{\bar{q}}]\}_1$ and $\lambda \in \{+,-\}$. By induction on the number of free parameters and by varying $q \in Q(n-1,k)$, we prove the following theorem which generalizes Theorem 4.1 for $k > n$.

THEOREM 4.2. *If $A(p)$ is nonsingular for all $p \in [p]$, then*

$$(4.2) \qquad \partial\Sigma^p \subseteq \bigcup_{q\in Q(n-1,k)} \bigcup_{u\in U(k-n+1)} x(p_q,p_{\bar{q}}^u)\big|_{p_q\in[p_q]} \subseteq \Sigma^p.$$

The set in the middle of the relation (4.2) will be called set of end-point parametric hypersurfaces.

EXAMPLE 4.2. *Consider the parametric linear system*

$$\begin{pmatrix} 1 & p_1 \\ p_1 & p_2 \end{pmatrix} \cdot x = \begin{pmatrix} p_3 \\ p_3 \end{pmatrix}, \qquad \begin{array}{l} p_1 \in [0,1] \\ p_2 \in [-4,-1] \\ p_3 \in [0,2]. \end{array}$$

For the parameters varying within their intervals, $A(p)$ is nonsingular and

$$A^{-1}(p) = \begin{pmatrix} p_2 & -p_1 \\ -p_1 & 1 \end{pmatrix} / \left(-p_1^2 + p_2\right).$$

$Q(n-1,k) = \{\{1\},\{2\},\{3\}\}$, then we obtain the following set of PHS-s. For $q = \{1\}$ the corresponding end-point PHS-s are

$$x(p_1,p_2^-,p_3^-) = x(p_1,p_2^+,p_3^-) = (0,0)^\top,$$

$$x(p_1,p_2^-,p_3^+) = \begin{pmatrix} 8+2p_1 \\ -2+2p_1 \end{pmatrix} / (4+p_1^2),$$

$$x(p_1,p_2^+,p_3^+) = \begin{pmatrix} 2+2p_1 \\ -2+2p_1 \end{pmatrix} / (1+p_1^2).$$

Parts of these PHS-s corresponding to $p_1 \in [0,1]$ are presented on Figure 4.2A. For $q = \{2\}$ the corresponding end-point PHS-s are

$$x(p_2,p_1^-,p_3^-) = x(p_2,p_1^+,p_3^-) = (0,0)^\top,$$

$$x(p_2,p_1^-,p_3^+) = (2,2/p_2)^\top, \quad x(p_2,p_1^+,p_3^+) = (2,0)^\top.$$

Those parts of the above PHS-s corresponding to $p_2 \in [-4,-1]$ are presented on Figure 4.2B. For $q = \{3\}$ the corresponding end-point PHS-s are

$$x(p_3,p_1^-,p_2^-) = (p_3,-p_3/4)^\top, \quad x(p_3,p_1^+,p_2^-) = x(p_3,p_1^-,p_2^+) = (p_3,0)^\top,$$
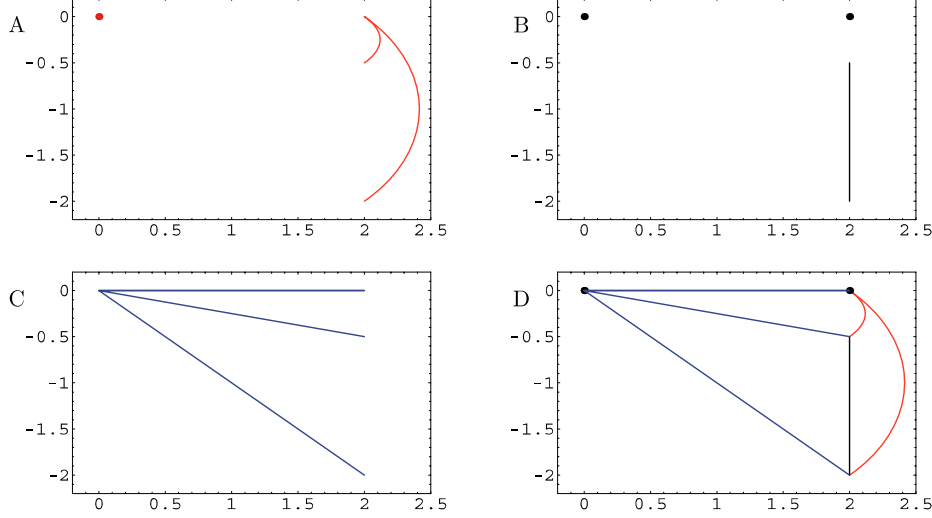
$$x(p_3,p_1^-,p_2^+) = (p_3,-p_3)^\top.$$

Figure 4.2: Parts of the end-point parametric hypersurfaces for the system from Example 4.2. A: $x(p_1, p_{\bar{1}}^u)|_{p_1 \in [0,1]}$, B: $x(p_2, p_{\bar{2}}^u)|_{p_2 \in [-4,-1]}$, C: $x(p_3, p_{\bar{3}}^u)|_{p_3 \in [0,2]}$, where $u \in U(2)$. D: The parametric solution set represented by the set of all end-point parametric hypersurfaces for the system from Example 4.2.

Those parts of the above PHS-s corresponding to $p_3 \in [0,2]$ are presented on Figure 4.2C. The set of all end-point PHS-s restricted to the ranges of the corresponding parameters is presented on Figure 4.2D.

The set of all end-point PHS-s contains superfluous parametric hypersurfaces (those which do not belong to the boundary). The dimension of this set is also quite big, $\mathrm{Card}(\bigcup_{q \in Q} \bigcup_{u \in U} x(p_q, p_{\bar{q}}^u)) = \binom{k}{n-1} 2^{k-n+1}$, growing with the dimension of the system and the number of free parameters. In the 3D case drawing superfluous parametric surfaces will make the plotting function take much longer to render the surface. Therefore, we need a mechanism for filtering only the boundary PHS-s from the set of all end-point parametric hypersurfaces. Since Remark 4.1 remains valid also for $k > n$, all degenerate end-point PHS-s may be eliminated from the set of end-point PHS-s. One criterion for eliminating particular end-point PHS-s is given by the following theorem where $\square$ denotes the interval hull defined by $\square S := [\inf S, \sup S]$ for a nonempty bounded set $S \subseteq \mathbb{R}^n$.

THEOREM 4.3. *Let $A(p)$ be nonsingular for all $p \in [p]$ and $k > n$. For fixed $q \in Q(n-1, k)$ and $\lambda \in U(k-n+1)$, the corresponding restricted PHS $x(p_q, p_{\bar{q}}^\lambda)|_{p_q \in [p_q]}$ does not belong to $\partial \Sigma^p$ if there exists another piece of PHS, defined by $r \in Q(n-1, k)$ and $\mu \in U(k-n+1)$, such that*

$$\square x(p_q, p_{\bar{q}}^\lambda)\big|_{p_q \in [p_q]} \subset \square x(p_r, p_{\bar{r}}^\mu)\big|_{p_r \in [p_r]} \neq \square \Sigma^p.$$

PROOF. For $r = q$, the coordinate functions of $x(p_q, p_{\bar{q}}^\lambda)$ depend on the same parameters for all $\lambda \in U(k-n+1)$ and therefore the inclusion means that

$x(p_q, p_{\bar{q}}^{\lambda})|_{p_q \in [p_q]}$ belongs to the interior of Σ^p. For $r \neq q$, the inequality and proper inclusion relations prevent from excluding boundary PHS-s contributing to the solution set hull. □

EXAMPLE 4.3. *Consider the parametric linear system*

$$\begin{pmatrix} 2p_1 & -p_2 \\ p_2 & 2p_1 \end{pmatrix} \cdot x = \begin{pmatrix} p_3 \\ p_3 \end{pmatrix}, \qquad \begin{array}{l} p_1 \in [1, 2] \\ p_2 \in [-1.2, 2] \\ p_3 \in [-2, 2]. \end{array}$$

The matrix is nonsingular for all values of the parameters within their intervals and

$$A^{-1}(p) = \begin{pmatrix} 2p_1 & p_2 \\ -p_2 & 2p_1 \end{pmatrix} / (4p_1^2 + p_2^2).$$

$Q(n-1, k) = \{\{1\}, \{2\}, \{3\}\}$, then we obtain the following set of end-point PHS-s. For $q = \{1\}$

$$x(p_1, p_2^-, p_3^-) = -x(p_1, p_2^-, p_3^+) = \begin{pmatrix} 15 - 25p_1 \\ -15 - 25p_1 \end{pmatrix} / (9 + 25p_1^2),$$

$$x(p_1, p_2^+, p_3^-) = -x(p_1, p_2^+, p_3^+) = \begin{pmatrix} -1 - p_1 \\ 1 - p_1 \end{pmatrix} / (1 + p_1^2).$$

The corresponding pieces of these PHS-s are presented on Figure 4.3A. For their hulls we have

$$\square x(p_1, p_2^-, p_3^-)|_{p_1 \in [p_1]} = \begin{pmatrix} \left[\frac{-5}{6 + 6\sqrt{2}}, \frac{-5}{17} \right] \\ \left[\frac{-20}{17}, \frac{-65}{109} \right] \end{pmatrix},$$

$$\square x(p_1, p_2^+, p_3^-)|_{p_1 \in [p_1]} = \begin{pmatrix} [-1, -3/5] \\ [-1/5, 0] \end{pmatrix}.$$

For $q = \{1\}$ no one of the restricted PHS-s satisfies Theorem 4.3.

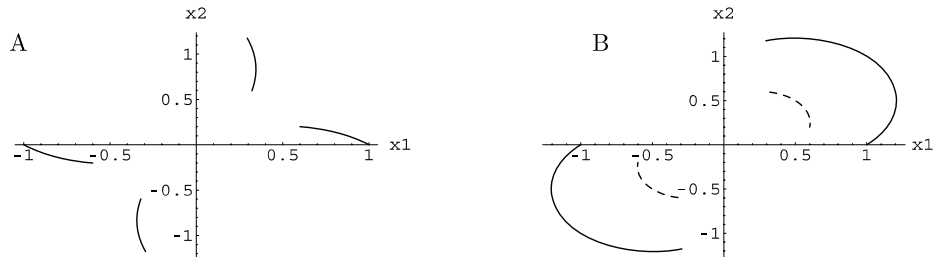Figure 4.3: Restricted end-point PHS-s for the system from Example 4.3 and $q = \{1\}$ (A), $q = \{2\}$ (B).

For $q = \{2\}$,

$$x(p_1^-, p_2, p_3^-) = -x(p_1^-, p_2, p_3^+) = \begin{pmatrix} -4 - 2p_2 \\ -4 + 2p_2 \end{pmatrix} / \left(4 + p_2^2\right),$$

$$x(p_1^+, p_2, p_3^-) = -x(p_1^+, p_2, p_3^+) = \begin{pmatrix} -8 - 2p_2 \\ -8 + 2p_2 \end{pmatrix} / \left(16 + p_2^2\right).$$

The corresponding pieces of these PHS-s are presented on Figure 4.3B. For their hulls we have

$$\Box x(p_1^-, p_2, p_3^-)|_{p_2 \in [p_2]} = \begin{pmatrix} \left[\frac{1}{\sqrt{2}(-2+\sqrt{2})}, \frac{-5}{17}\right] \\ \left[\frac{1}{\sqrt{2}(-2+\sqrt{2})}, 0\right] \end{pmatrix},$$

$$\Box x(p_1^+, p_2, p_3^-)|_{p_2 \in [p_2]} = \begin{pmatrix} \left[\frac{1}{4-4\sqrt{2}}, \frac{-35}{109}\right] \\ \left[\frac{-65}{109}, \frac{-1}{5}\right] \end{pmatrix}.$$

Since $\Box x(p_1^+, p_2, p_3^-)|_{p_2 \in [p_2]} \subset \Box x(p_1^-, p_2, p_3^-)|_{p_2 \in [p_2]}$, by Theorem 4.3, $x(p_1^+, p_2, p_3^-)|_{p_2 \in [p_2]}$ is not a boundary curve. Analogously $x(p_1^-, p_2, p_3^+)|_{p_2 \in [p_2]}$ is not a boundary curve. Both curves are represented on Figure 4.3B as dashed curves. For $q = \{3\}$,

$$x(p_1^-, p_2^-, p_3) = \begin{pmatrix} 5p_3/34 \\ 10p_3/17 \end{pmatrix}, \quad x(p_1^+, p_2^-, p_3) = \begin{pmatrix} 35p_3/218 \\ 65p_3/218 \end{pmatrix}$$

$$x(p_1^-, p_2^+, p_3) = \begin{pmatrix} p_3/2 \\ 0 \end{pmatrix}, \quad x(p_1^+, p_2^+, p_3) = \begin{pmatrix} 3p_3/10 \\ p_3/10 \end{pmatrix}.$$

The corresponding pieces of these PHS-s are presented on Figure 4.4A and their hulls are

$$\Box x(p_1^-, p_2^-, p_3)|_{p_3 \in [p_3]} = \begin{pmatrix} \left[\frac{-5}{17}, \frac{5}{17}\right] \\ \left[\frac{-20}{17}, \frac{20}{17}\right] \end{pmatrix}, \quad \Box x(p_1^+, p_2^-, p_3)|_{p_3 \in [p_3]} = \begin{pmatrix} \left[\frac{-35}{109}, \frac{35}{109}\right] \\ \left[\frac{-65}{109}, \frac{65}{109}\right] \end{pmatrix}$$

$$\Box x(p_1^-, p_2^+, p_3)|_{p_3 \in [p_3]} = \begin{pmatrix} [-1, 1] \\ [0, 0] \end{pmatrix}, \quad \Box x(p_1^+, p_2^+, p_3)|_{p_3 \in [p_3]} = \begin{pmatrix} \left[\frac{-3}{5}, \frac{3}{5}\right] \\ \left[\frac{-1}{5}, \frac{1}{5}\right] \end{pmatrix}.$$

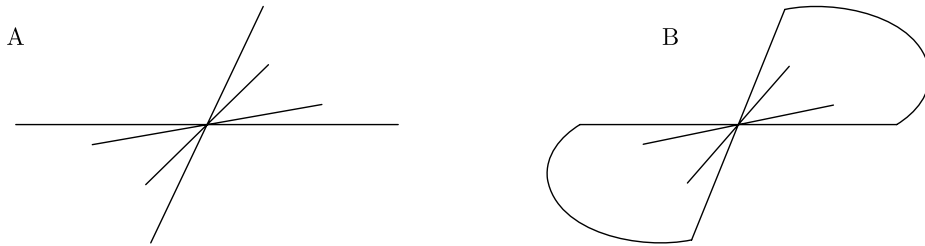For $q = \{3\}$ no one of the restricted PHS-s satisfies Theorem 4.3.

Figure 4.4: For the system from Example 4.3, A: end-point PHS-s for $q = \{3\}$; B: the set of end-point PHS-s for $q = \{1\}, \{2\}, \{3\}$ after the application of Theorem 4.3.

Since both $\square x(p_1, p_2^-, p_3^-)|_{p_1 \in [p_1]}$, $\square x(p_1, p_2^+, p_3^-)|_{p_1 \in [p_1]}$ are contained in $\square x(p_1^-, p_2, p_3^-)|_{p_2 \in [p_2]}$ and both $\square x(p_1, p_2^-, p_3^+)|_{p_1 \in [p_1]}$, $\square x(p_1, p_2^+, p_3^+)|_{p_1 \in [p_1]}$ are contained in $\square x(p_1^-, p_2, p_3^+)|_{p_2 \in [p_2]}$, then by Theorem 4.3 all restricted PHS-s for $q = \{1\}$ are not boundary curves. The set of restricted end-point PHS-s that remains after the application of Theorem 4.3 is drawn on Figure 4.4B. Obviously, there are end-point PHS-s that do not belong to the boundary but cannot be eliminated by the above criterion. For producing a best looking graphics the superfluous end-point PHS-s can be eliminated manually by enumerating the elements of the set of end-point parametric hypersurfaces.

5 2D projections of practical examples.

In this section we present some larger and practical examples further illustrating the application of the discussed methodology. The first example illustrates the application of Theorem 4.1 for visualization of a 3D parametric solution set. Then, next two examples come from practical models of electrical circuits. These examples demonstrate the application of Theorem 4.2 and the efficacy of the discussed approach for visualizing parametric solution sets of higher dimensions and depending on many uncertain parameters. All graphics images are generated automatically in the environment of *Mathematica* [20] by newly developed functions implementing the presented methodology.

EXAMPLE 5.1. *Consider the following 3D linear system*

$$\begin{pmatrix} 1 & p_1 & p_2 \\ p_1 & 2 & p_1 \\ p_2 & p_1 & 3 \end{pmatrix} \cdot x = \begin{pmatrix} 1 - p_3 \\ p_3/3 + 1 \\ p_3/2 \end{pmatrix}, \qquad \begin{matrix} p_1 \in [-1/2, 1] \\ p_2 \in [-1/2, 1/2] \\ p_3 \in [0, 1]. \end{matrix}$$

Since the number of the parameters is equal to the dimension of the system, according to Theorem 4.1, the boundary of the parametric solution set to the above system is exactly representable by at most six restricted PHS-s in the 3D space. The corresponding graphics is presented in an electronic supplementary material as a pdf file and an active *Mathematica* notebook. One can open the notebook by the free *Mathematica* Player [21] in order to have the best view of the parametric solution set by rotating, scaling and zooming the graphics in real-time. The shape of the solution set can be also seen in a web page

http://cose.math.bas.bg/webMathematica/3Dex-ParSSet.jsp

where the applet LiveGraphics3D [13] enables everyone with a web browser supporting Java to view and interactively rotate the graphics.

For 3D systems involving more parameters than the dimension of the system, rendering the whole set of 3D end-point restricted PHS-s will be too heavy. In such cases and also for larger systems, a good impression about the parametric solution set can be obtained via its 2D projections. Taking two desired components of the analytic system solution we obtain a 2D parametric solution set projecting the original one onto the corresponding coordinate plane. The latter

2D parametric projection set is visualized according to Theorem 4.2 by generating and drawing all end-point restricted parametric curves. Figure 5.1 represents the set of end-point restricted parametric curves projecting the solution set of the system from Example 5.1 on the plane x_2, x_3. It seems that the projection on this coordinate plane gives the best impression of the example 3D parametric solution set. Most of the restricted end-point parametric curves at least partially form the boundary of the projection. Some end-point parametric curves show non-monotonic dependence on the parameter.
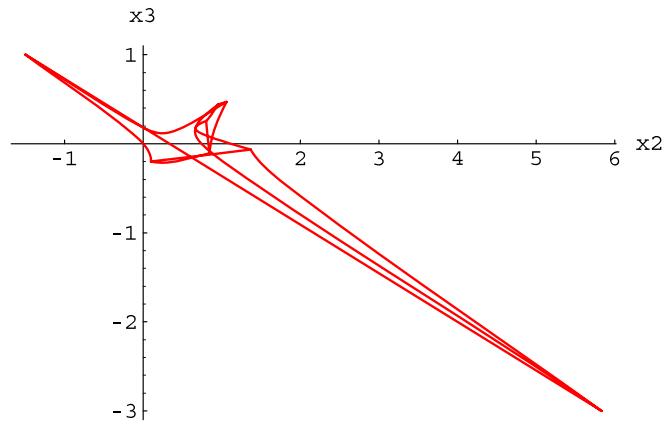

Figure 5.1: Projection of the 3D parametric solution set from Example 5.1 on the plane x_2, x_3.

The application of Kichhoff's laws to planar resistive networks with uncertain resistances leads to parametric linear systems. Below we consider two such systems of dimension 5 and apply the proposed methodology for plotting projections of the parametric solution set on particular coordinate planes.

EXAMPLE 5.2. *Consider the resistive network presented in Figure 5.2. After the considerations in* [10], *the output voltage V_{out} is obtained via solution of the following linear equations*

$$\begin{pmatrix} 30 & -10 & -10 & -10 & 0 \\ -10 & 10+\theta_2+\theta_1 & -\theta_1 & 0 & 0 \\ -10 & -\theta_1 & 15+\theta_3+\theta_1 & -5 & 0 \\ -10 & 0 & -5 & 15+\theta_4 & 0 \\ 0 & 0 & -5 & 5 & 1 \end{pmatrix} \cdot \begin{pmatrix} x_1 \\ x_2 \\ x_3 \\ x_4 \\ x_5 \end{pmatrix} = \begin{pmatrix} 1 \\ 0 \\ 0 \\ 0 \\ 0 \end{pmatrix},$$

where the i-th solution variable x_i is taken to be the current I_i, $i = 1, 2, 3, 4$ and $x_5 = V_{out}$, while the resistances are associated with the parameters θ_j. Assuming resistances θ_j with nominal values $\theta_1^0 = 10\Omega$, $\theta_2^0 = 6\Omega$, $\theta_3^0 = 10\Omega$, $\theta_4^0 = 10\Omega$, and that each θ_j lies within $\pm 2\Omega$ of its nominal value, we are interested to represent the set of system responses whenever the parameters vary within the box $[8, 12] \times [4, 8] \times [8, 12] \times [8, 12]$.
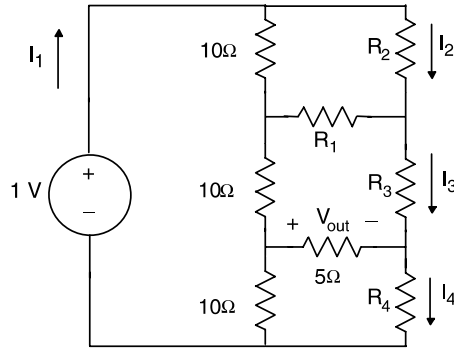
Figure 5.2: Example electrical circuit, after [10].

In this example the number of the parameters is less than the number of the variables. Although the boundary of the parametric solution set is exactly representable by PHS-s in the 5D space we can visualize only its 2D projections. In order to see what is the variation of the output voltage V_{out} $(= x_5)$ under the specified variations in the resistances, we choose a projection onto the plane x_4, x_5, Figure 5.3. With respect to each parameter there are eight end-point parametric curves, see Figure 5.3B. All of them are linear for this example, a property that corresponds to monotonic dependencies proven in [10] by another method. Identifying which lines are on the boundary can be easily done if sorting each set of end-point PHS-s in a canonical order of the points building the curves. Thus the boundary presented in Figure 5.3. A consists of the curves with number 1 and 7 (w.r.t. θ_1), 4 and 6 (w.r.t. θ_2), 2 and 7 (w.r.t. θ_3), 1 and 8 (w.r.t. θ_4), compare to Figure 5.3B.
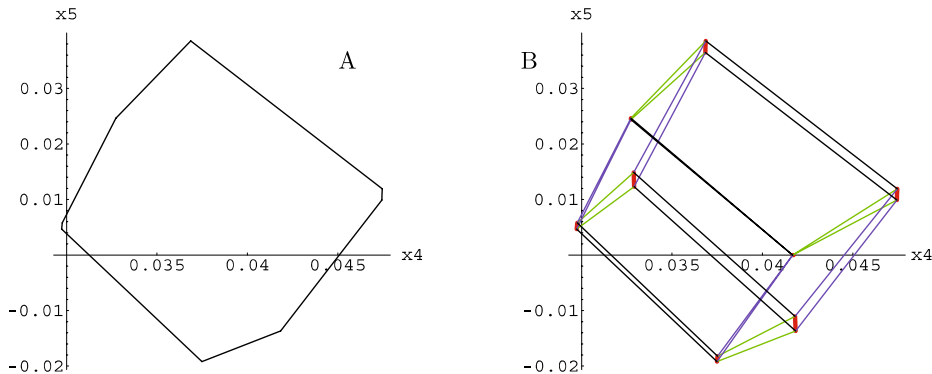

Figure 5.3: Projection of the parametric solution set from Example 5.2 on the plane x_4, x_5. A: boundary curves, B: the set of end-point parametric curves w.r.t. θ_1, θ_2, θ_3, θ_4.

EXAMPLE 5.3. *Consider the so-called Okumura's problem. This is a linear resistive network, presented in* [16] *and considered also in* [17]. *The resistive*

network consists of two current sources J_1 and J_2 and nine resistors. The problem of finding the voltages $v_1, \ldots, v_5$, when the voltage of each conductance $g_i, i = 1, \ldots, 9$ varies independently in prescribed bounds $[g_i]$, leads to the following parametric linear system

$$(5.1) \quad \begin{pmatrix} g_1 + g_6 & -g_6 & 0 & 0 & 0 \\ -g_6 & g_2 + g_6 + g_7 & -g_7 & 0 & 0 \\ 0 & -g_7 & g_3 + g_7 + g_8 & -g_8 & 0 \\ 0 & 0 & -g_8 & g_4 + g_8 + g_9 & -g_9 \\ 0 & 0 & 0 & -g_9 & g_5 + g_9 \end{pmatrix} v = J,$$

where $J = (10, 0, 10, 0, 0)^\top$. The parameters g_i, $i = 1, \ldots, 9$ are subject to tolerance $\delta = 0.01$, that is $g_i \in [1 - \delta, 1 + \delta]$.

Figure 5.4 presents the projection of the parametric solution set on the plane of the first two coordinates.
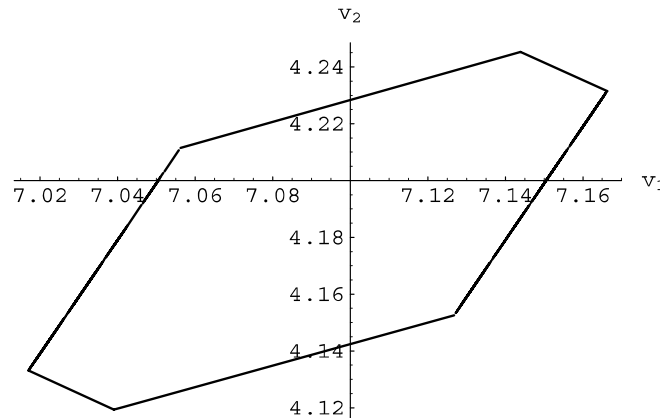

Figure 5.4: Projection of the parametric solution set from Example 5.3 on the v_1, v_2-plane.

This example involves more parameters than the previous one. For each parameter, the set of end-point PHS-s involves 256 curves which makes the process of eliminating the PHS-s, that are not on the boundary, more difficult. The set of end-point PHS-s for g_6 is such that the first and the last curves in the canonical order of the set are on the boundary of the parametric solution set, see Figure 5.5A. Since in this example there is again a monotonic dependence of the solution on the parameters, the canonical order of the curves in the set of end-point PHS-s helps to find which are the boundary curves, i.e. these are curves number 73 and 184 for g_1. For all other parameters, the sets of end-point PHS-s consist of many small line segments located on same lines and boundary-lines, see e.g. Figure 5.5B presenting in black the set of end-point PHS-s for g_9. Line segments with the following numbers 1–40, 56, 65–69, 86, 65–55, 171, 172, 176, 178–180,

185–192, 201–204, 217–256, in the canonical order of the set of PHS-s for g_7, are boundary segments used in the plot of Figure 5.4.
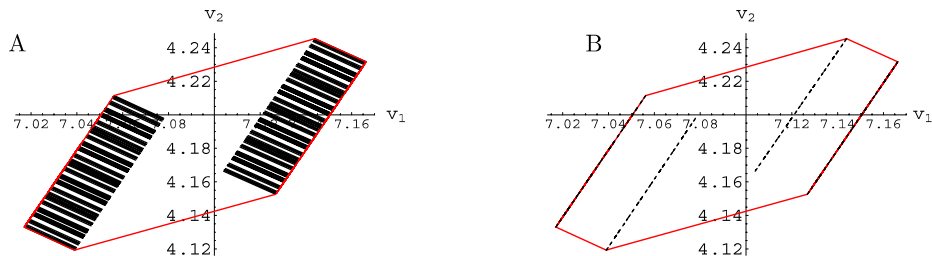

Figure 5.5: Projection of the parametric solution set from Example 5.3 on the v_1, v_2-plane and: the set of all end-point PHS-s for g_6 (A), the set of all end-point PHS-s for g_9 (B).

6 Conclusion.

We characterized the boundary of a parametric solution set by parts of parametric hypersurfaces. In view that some environments like *Mathematica* and Maple support tools for drawing parametric hypersurfaces, the presented approach is much more straightforward for visualization of parametric solution sets (and their projections) than the approach based on a combination of Fourier–Motzkin like elimination and CAD for visualization of inequalities. The methodology presented in this paper is applicable for visualizing the parametric solution set of any linear system whose solution can be computed analytically. The overall amount of work can be distributed because the set of end-point parametric hypersurfaces can be handled separately for each parameter. Furthermore, this is the only approach for visualizing the solution set when $k \leq n - 1$ since the inequalities plotting functions cannot visualize equations.

Acknowledgments.

The authors thank Prof. L. Eldén and the two anonymous referees for their valuable suggestions and remarks which improved this paper.

REFERENCES

1. J. Ackermann, A. Bartlett, D. Kesbauer, W. Sienel, and R. Steinhauser, *Robust Control: Systems with Uncertain Physical Parameters*, Springer, Berlin, 1994.

2. B. R. Barmish, *New Tools for Robustness of Linear Systems*, MacMillan, New York, 1994.

3. M. S. Baouendi, P. Ebenfelt, L. P. Rothschild, *Real Submanifolds in Complex Space and Their Mappings*, Princeton Univ. Press, Princeton, New Jersey, 1999.

4. G. Alefeld, V. Kreinovich, and G. Mayer, *On the shape of the symmetric, persymmetric, and skew-symmetric solution set*, SIAM J. Matrix Anal. Appl., 18(3) (1997), pp. 693–705.

5. G. Alefeld, V. Kreinovich, and G. Mayer, *The shape of the solution set for systems of interval linear equations with dependent coefficients*, Math. Nachr., 192 (1998), pp. 23–36.

6. G. Alefeld, V. Kreinovich, and G. Mayer, *On symmetric solution sets*, Comput. Suppl., 16 (2002), pp. 1–22.

7. G. Alefeld, V. Kreinovich, and G. Mayer, *On the solution sets of particular classes of linear interval systems*, J. Comput. Appl. Math., 152 (2003), pp. 1–15.

8. S. Boyd, L. Vandenberghe, *Convex Optimization*, Cambridge University Press, Cambridge, 2004.

9. G. E. Collins, *Quantifier elimination by cylindrical algebraic decomposition – twenty years of progress*, in B. F. Caviness and J. R. Johnson (eds.), Quantifier Elimination and Cylindrical Algebraic Decomposition, Springer, New York, 1998, pp. 8–23.

10. A. Ganesan, S. Ross, B. Ross Barmish, *An extreme point result for convexity, concavity and monotonicity of parametrized linear equation solutions*, Linear Algebra Appl., 390 (2004), pp. 61–73.

11. M. Kofler, *Maple: An Introduction and Reference*, Addison-Wesley, Reading, MA, 1997.

12. W. Krämer, *Computing and visualizing the exact solution set of systems of equations with interval coefficients*, in 12th International Conference on Applications of Computer Algebra (ACA'06), June 26–29, 2006, Varna, Bulgaria.

13. M. Kraus, *LiveGraphics3D: a Java applet which can display Mathematica graphics*, http://www.vis.uni-stuttgart.de/∼kraus/LiveGraphics3D/.

14. R. L. Muhannah, R. L. Mullen (eds.), in Proceedings of the NSF Workshop on Reliable Engineering Computing, Svannah, Georgia USA, Feb. 22–24, 2006, http://www.gtsav.gatech.edu/workshop/rec06/proceedings.html.

15. W. Oettli, W. Prager, *Compatibility of approximate solution of linear equations with given error bounds for coefficients and right-hand sides*, Numer. Math., 6 (1964), pp. 405–409.

16. K. Okumura, *An application of interval operations to electric network analysis*, Bull. Japan Soc. Industr. Appl. Math., 2 (1993), pp. 115–127.

17. E. Popova, *On the solution of parametrised linear systems*, in W. Krämer, J. Wolff von Gudenberg (eds.), Scientific Computing, Validated Numerics, Interval Methods, Kluwer Acad. Publishers, Boston, Dordrecht, London, 2001, pp. 127–138.

18. E. Popova, *Web-accessible tools for interval linear systems*, Proc. Appl. Math. Mech. (PAMM), 5(1) (2005), pp. 713–714.

19. M. Spivak, *A Comprehensive Introduction to Differential Geometry*, four volumes, 2nd edn., Publish or Perish Inc., Berkeley, 1979.

20. S. Wolfram, *The Mathematica Book*, 4th edn., Wolfram Media/Cambridge U. Press, New York, 1999.

21. Wolfram Res. Inc., *The Mathematica Player*, 2007 (http://www.wolfram.com/products/player).